Target Detection in ISAC System Equipped with IRS: A Joint Active and Passive Beamforming Approach

Safa Awad[1], Rui Wang[1(✉)], and Ismael Soto[2]

[1] College of Electronics and Information Engineering, Tongji University, Shanghai 201804, China
{safa,ruiwang}@tongji.edu.cn

[2] Department Electrical Engineering, University of Santiago, 3519 Santiago de Chile, AE, Chile
ismael.soto@usach.cl

Abstract. To explore the use of intelligent reflecting surface (IRS) technology to improve target detection in an integrated sensing and communication (ISAC) system, this paper investigates the joint active and passive beamforming design for ISAC system equipped with IRS. An optimization problem is formulated to maximize the signal-to-noise ratio (SNR) at the base station (BS) while ensuring a minimum signal-to-interference-plus-noise-ratio (SINR) at each communication user (CU). An alternative algorithm is proposed to tackle this non-convex problem, and the problem is decomposed into three sub-problems. In the first sub-problem, the semi-definite relaxation (SDR) algorithm is used to solve the communication and sensing beamformers. A receive combining vector at the base station is derived from an equivalent Rayleigh-quotient problem in the second sub-problem. Lastly, the Successive Convex Approximation (SCA) based algorithm is applied to yield the IRS phase shift solution in the third sub-problem. The optimization algorithm alternates between these three steps until convergence is achieved. Simulation results demonstrate the effectiveness of the proposed beamforming algorithm, showcasing its superiority over the matched filter (MF) approach.

Keywords: Integrated sensing and communication (ISAC) · Intelligent reflecting surface (IRS) · Active and passive beamforming optimization

1 Introduction

In recent years, the integration of intelligent reflecting surfaces (IRS), also called reconfigurable intelligent surfaces (RIS) into wireless communication systems has shown great potential in enhancing system performance and enabling new capabilities [1]. IRS is a programmable surface consisting of many passive reflecting elements, which can collectively perform various functions to manipulate and control electromagnetic waves (EW) [2]. However, the escalating demand for wireless communication services, such as the proliferation of Internet of Things (IoT) devices, the increasing adoption of cloud computing, and the development of smart cities and connected infrastructure, has resulted

F. Gao et al. (Eds.): Chinacom 2023, LNICST 590, pp. 66–80, 2024.
https://doi.org/10.1007/978-3-031-67162-3_5

in a crowded and scarce frequency spectrum [3]. To address this challenge, integrated sensing and communication (ISAC) systems have emerged, enabling efficient spectrum utilization by combining sensing and communication functionalities, allowing them to share the same frequency bands [4] simultaneously. The ISAC system offers a cost-effective solution for applications where both sensing and communication functions are required, including autonomous vehicles (AVs) [5], unmanned aerial systems (UAS), or military surveillance systems. The integration of RIS with ISAC systems has captured many researchers' attention due to its numerous benefits. The authors of [6] proposed a joint design of transmit beamforming and RIS to maximize the radar signal-to-noise ratio (SNR) as a performance metric of target estimation. In [7], the authors investigated the use of RIS to mitigate multi-user interference while synthesizing a desired transmit beam pattern and optimizing the DFRC waveform and RIS phase shift matrix. In this article [8], the authors proposed a novel ISAC-RIS system that utilizes a dual-function base station to transmit the superimposed non-orthogonal multiple access (NOMA) communication signals to serve both communication users and sensing targets concurrently.

In this work, our objective is to maximize the signal-to-noise ratio at the base station to enhance target detection by jointly optimizing the communication and sensing beamformers. The problem is highly non-convex due to the deeply coupled variables and the unit-modulus phase shift constraint. To tackle this problem, we propose an alternative optimization approach in which the communication and sensing beamformers are optimized using the SDR algorithm. The receive combining vector is optimized based on an equivalent Rayleigh-quotient problem. For the passive beamformer, we used a real-valued first-order Taylor expansion to linearize the objective function, and the SCA-based algorithm is designed to find the IRS phase shift solution. In this paper, the target is considered to be unknown, but it is expected to be within the range (0, r] in terms of distance, where r is the distance between a possible target and the IRS, and within the regions $[\vartheta_1, \vartheta_2]$ and $[\varphi_1, \varphi_1]$ for elevation angle-of-departure (AOD) and azimuth AOD from the IRS to the possible target, respectively. The sensing and communication tasks are executed simultaneously. The IRS reflects the beamformers emitted by the base station toward the communication users and potential targets. The presence of a target is determined by reflecting a portion of the scattered wave, which is dispersed throughout the propagation space when the reflective beam illuminates the target. The reflected wave, known as the echo, is then redirected back to the BS by the IRS and received for further processing to detect the target. Simulation results validate the efficiency of our optimization approach, highlighting its ability to achieve remarkable SNR gains at the BS. The remaining sections of this paper are structured as follows. Section 2 introduces the IRS-aided ISAC system model and formulates the maximization problem. The communication and the sensing metrics will also be discussed in this section. An optimization algorithm is proposed in Sect. 3 to solve the optimization problem. Simulation results are provided in Sect. 4. Finally, Sect. 5 concludes this paper.

2 System Model and Problem Formulation

2.1 System Model

In this scenario, we consider a multicast wireless downlink communication system with a base station with M transmitting and receiving antennas organized in a uniform linear array (ULAs) and d antenna spacing. IRS with N reflecting elements arranged in a uniform planner array (UPAs) with N_x and N_y Elements per dimension, respectively. Single-antenna communication users denoted by $k \in \mathcal{K} = \{1, ..., K\}$, , and assumed to be static. A target that needs to be detected does not have a direct line-of-sight (LOS) path from the BS, as illustrated in Fig. 1.

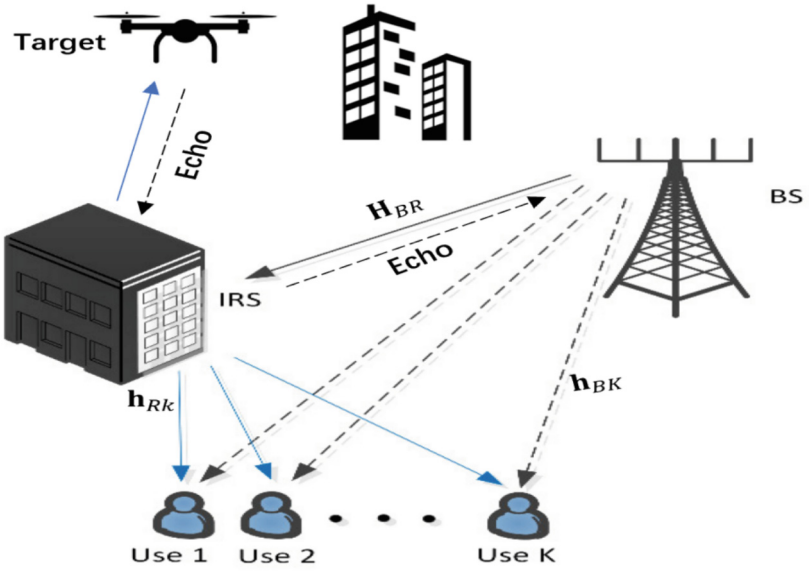

Fig. 1. An IRS-assisted ISAC system.

Communication Metric. The transmitted waveform at the BS serves both communications and sensing purposes and can be denoted by

$$\mathbf{x}(t) = \mathbf{w_c} s_c(t) + \mathbf{w}_r s_r(t)$$

where $\mathbf{w}_c \in \mathbb{C}^{M\times 1}$ and $\mathbf{w}_r \in \mathbb{C}^{M\times 1}$ are the active communication and sensing beamformer vectors, respectively. The communication signal $s_c(t)$ and the sensing signal $s_r(t)$ are assumed to be statistically independent of each other and uncorrelated, satisfying $\mathbb{E}\{s_r(t)s_c(t)^*\} = 0$, and $\mathbb{E}\big(s_r(t)s_r(t)^{\mathrm{H}}\big) = \mathbb{E}\big(s_c(t)s_c(t)^{\mathrm{H}}\big) = 1$.

The received signal at the k-th communication receivers can be expressed as.

$$y_k = \left[\mathbf{h}_{Rk}^{\mathrm{H}} \boldsymbol{\Theta}(\boldsymbol{\Psi}_R, \boldsymbol{\Psi}_k)\mathbf{H}_{BR} + \mathbf{h}_{Bk}^{\mathrm{H}}\right]\mathbf{x}(t) + n_k(t), \forall k \in \mathcal{K}, \tag{1}$$

where $\mathbf{H}_{BR} \in \mathbb{C}^{N\times M}$, $\mathbf{h}_{Rk} \in \mathbb{C}^{N\times 1}$, and $\mathbf{h}_{Bk} \in \mathbb{C}^{M\times 1}$ denote the BS-IRS channel, IRS-k user channel, and BS-k user channel,$\forall k \in \mathcal{K}$, respectively. The diagonal IRS response matrix with respect to the incident direction $\mathbf{\Psi}_R$ and the k-th users' direction $\mathbf{\Psi}_k$, which can be expressed as $\mathbf{\Theta}(\mathbf{\Psi}_R, \mathbf{\Psi}_k) = \text{diag}(\boldsymbol{\phi})$, where $\boldsymbol{\phi}$ represents the unite modulus phase shift vector that satisfies $\boldsymbol{\phi} = \left[e^{j\theta_1}, ..., e^{j\theta_N}\right]^{\mathrm{T}}$, where θ_n represents the phase shift reflection coefficient of the IRS elements, for $n = 1, 2, ..., N$, being the phase shift variables. $n_k(t) \sim \mathcal{CN}\left(0, \sigma_k^2\right)$ denotes the additive white Gaussian noise (AWGN) at the k-th users with σ_k^2 being the noise power.

Channel Model. In our scenario, we assume a perfect channel state information (CSI) of the channels, which can be acquired using various channel estimation methods [9], and they are modeled as.

$$\mathbf{H}_{BR} = \sqrt{\frac{PL_{BR}^{\kappa}}{1+\kappa}}\overline{\mathbf{H}}_{BR} + \sqrt{\frac{PL_{BR}}{1+\kappa}}\tilde{\mathbf{H}}_{BR}, \tag{2}$$

where κ is the Rician factor, and the large-scale path loss is given by.

$$PL_{BR} = L_0\left(\frac{d_{BR}}{d_0}\right)^{-\alpha BR}, \tag{3}$$

where L_0 is the path loss coefficient at $d_0 = 1$ m, and αBR is the path loss exponent while d_{BR} denotes the distance between the BS and the IRS, the same equation is applied to the remaining channels. $\tilde{\mathbf{H}}_{BR}$ is the NLOS Rayleigh fading components, while the LOS components are represented by

$$\begin{gathered}\overline{\mathbf{H}}_{BR} = \mathbf{a}(\vartheta_R, \varphi_R)\mathbf{a}^{\mathrm{H}}(\vartheta_{BR}, \varphi_{BR}), \overline{\mathbf{h}}_{Rk} = \mathbf{a}(\vartheta_k, \varphi_k), \forall k \in \mathcal{K} \\ \overline{\mathbf{h}}_{Bk} = \mathbf{a}(\vartheta_{Bk}, \varphi_{Bk}), \forall k \in \mathcal{K}\end{gathered} \tag{4}$$

where ϑ_R and φ_R are the elevation and azimuth angle-of-arrivals (AOAs) at the IRS. The elevation and azimuth angle-of-departures (AODs) at the BS toward the IRS are ϑ_{BR} and φ_{BR}, and toward the k-th users are ϑ_{Bk} and φ_{Bk}. The steering vectors are expressed as

$$\begin{aligned}\mathbf{a}(\vartheta_{BX}, \varphi_{BX}) &= \left(1, e^{j\frac{2\pi d}{\lambda}sin\vartheta_{BX}sin\varphi_{BX}}, ..., e^{j\frac{2\pi d}{\lambda}(M-1)sin\vartheta_{BX}sin\varphi_{BX}}\right)^{\mathrm{T}}, X \in \{R, k\}, \\ &\forall k \in \mathcal{K} \\ \mathbf{a}(\vartheta_R, \varphi_R) &= \left(1, e^{j\frac{2\pi d}{\lambda}sin\vartheta_R cos\varphi_R}, ..., e^{j\frac{2\pi d}{\lambda}(N_x-1)sin\vartheta_R cos\varphi_R}\right)^{\mathrm{T}} \\ &\otimes \left(1, e^{j\frac{2\pi d}{\lambda}sin\vartheta_R sin\varphi_R}, ..., e^{j\frac{2\pi d}{\lambda}(N_y-1)sin\vartheta_R sin\varphi_R}\right)^{\mathrm{T}} \\ \mathbf{a}(\vartheta_k, \varphi_k) &= \left(1, e^{j\frac{2\pi d}{\lambda}sin\vartheta_k cos\varphi_k}, ..., e^{j\frac{2\pi d}{\lambda}(N_x-1)sin\vartheta_k cos\varphi_k}\right)^{\mathrm{T}} \\ &\otimes \left(1, e^{j\frac{2\pi d}{\lambda}sin\vartheta_k sin\varphi_k}, ..., e^{j\frac{2\pi d}{\lambda}(N_y-1)sin\vartheta_k sin\varphi_k}\right)^{\mathrm{T}}, \forall k \in \mathcal{K}.\end{aligned}$$

The SINR at the k-th users can be represented by.

$$\text{SINR}_k = \frac{\left|(\mathbf{h}_{Bk}^{\mathrm{H}} + \mathbf{h}_{Rk}^{\mathrm{H}}\mathbf{\Theta}(\mathbf{\Psi}_R, \mathbf{\Psi}_k)\mathbf{H}_{BR})\mathbf{w}_c\right|^2}{\left|(\mathbf{h}_{Bk}^{\mathrm{H}} + \mathbf{h}_{Rk}^{\mathrm{H}}\mathbf{\Theta}(\mathbf{\Psi}_R, \mathbf{\Psi}_k)\mathbf{H}_{BR})\mathbf{w}_r\right|^2 + \sigma_k^2}, \forall k \in \mathcal{K}. \tag{5}$$

Sensing Metric. The BS detects the presence of a target by analyzing the echo signal reflected back from it; the power of the echo signal can be mathematically derived as

$$\begin{aligned} E_s = \int_{\varphi_A-\frac{\Delta\varphi}{2}}^{\varphi_A+\frac{\Delta\varphi}{2}} \int_{\vartheta_A-\frac{\Delta\vartheta}{2}}^{\vartheta_A+\frac{\Delta\vartheta}{2}} \Big\{ & \frac{\lambda^2 \mathbb{E}\{L_1\}}{64\pi^3 r^2}\, \mathbf{a}^{\mathrm{H}}(\vartheta,\varphi) diag(\boldsymbol{\phi}) \mathbf{H}_{BR} \\ & \left(\mathbf{w}_c \mathbf{w}_c^{\mathrm{H}} + \mathbf{w}_r \mathbf{w}_r^{\mathrm{H}}\right) \mathbf{H}_{BR}^{\mathrm{H}} diag\left(\boldsymbol{\phi}^H\right) \mathbf{a}(\vartheta,\varphi) \\ & \mathbf{a}^{\mathrm{H}}(\vartheta,\varphi) diag\left(\boldsymbol{\phi}^{\mathrm{H}}\right) \mathbf{H}_{BR} \mathbf{w}_B \mathbf{w}_B^{\mathrm{H}} \mathbf{H}_{BR}^{\mathrm{H}} diag(\boldsymbol{\phi}) \\ & \mathbf{a}(\vartheta,\varphi) sin\vartheta \Big\}, d\vartheta\, d\varphi \end{aligned} \tag{6}$$

where L_1 signifies the average reduction or attenuation in signal strength that occurs due to the first-order scattering phenomenon and w_B is the receive combining vector at the BS. We build upon the derivation presented in [10]; interested readers may refer to the original paper for a detailed explanation.

The received SNR at the BS is given by

$$\mathrm{SNR} = \frac{Es}{\sigma_{\mathrm{r}}^2}, \tag{7}$$

where σ_{r}^2 is the noise power.

2.2 Problem Formulation

In this paper, we aim to maximize the SNR at the BS by optimizing both communication and sensing beamformer vectors, the receive combining vector at the BS, and the IRS phase-shift matrix. The problem can be stated as follow.

$$(\mathrm{P1}): \underset{\mathbf{w}_c, \mathbf{w}_r, \boldsymbol{\phi}, \mathbf{w}_B}{\text{maximize}}\ \mathrm{SNR}, \tag{8-a}$$

$$\text{subject to} \quad \mathrm{Tr}\left(\mathbf{w}_c \mathbf{w}_c^{\mathrm{H}}\right) + \mathrm{Tr}\left(\mathbf{w}_r \mathbf{w}_r^{\mathrm{H}}\right) \leq P_T, \tag{8-b}$$

$$\left|\boldsymbol{\phi}_n\right| = 1, n = 1, 2, ..., N, \tag{8-c}$$

$$\mathrm{SINR}_k \geq \gamma, \forall k \in \mathcal{K}, \tag{8-d}$$

$$\|\mathbf{w}_B\|_2 = 1, \tag{8-e}$$

in which (8-b) is the transmit power constraint, (8-c) is the phase-shift unit modulus constraint, in (8-d), γ is the threshold or the minimum SINR that is necessary for reliable communication, and (8-e) is the receive combing vector constraint. The objective function exhibits non-convexity, posing challenges in finding a local optimal solution. Consequently, an alternative iterative approach is devised to optimize the variables $\mathbf{w}_c$, $\mathbf{w}_r$, $\mathbf{w}_B$, and $\boldsymbol{\phi}$.

3 Optimization Algorithm

Undoubtedly, obtaining the optimal solution to the optimization problem is a challenging task. To address this, an alternative algorithm is designed; we first optimize the communication and sensing beamformers while the IRS phase-shit and the receive combining vector is fixed; with fixed communication and sensing beamformers and IRS phase-shit, an equivalent Rayleigh-quotient problem is proposed to optimize the receive combining vector, then we optimize the IRS phase-shift with fixed communication and sensing beamformers and the receive combining vector. By decomposing problem (P1) into three sub-problems, we can effectively handle the complexity of the overall problem while achieving enhanced performance in maximizing the SNR.

3.1 Optimize $\mathbf{w}_c$ and $\mathbf{w}_r$

With given $\boldsymbol{\phi}$ and $\mathbf{w}_B$, the optimization sub-problem can be written as

$$\text{(P2)}: \underset{\mathbf{w}_c, \mathbf{w}_r}{\text{maximize}}\ \text{SNR}, \tag{9-a}$$

$$\text{subject to (8}-\text{b), (8}-\text{d)}. \tag{9-b}$$

In order to tackle (P2), we will introduce two new matrices denoted as $\mathbf{C}$ and $\mathbf{X}_k$, in addition, we will utilize the trace to aid in solving this sub-problem, which can be reformulated as

$$\text{(P3)}: \underset{\mathbf{W}_c \succcurlyeq 0, \mathbf{W}_r \succcurlyeq 0}{\text{maximize}}\ \mu Tr(\mathbf{C}(\mathbf{W}_c + \mathbf{W}_r)), \tag{10-a}$$

$$\text{subject to}\quad \text{Tr}(\mathbf{X}_k \mathbf{W}_c) - \gamma\Big[\text{Tr}(\mathbf{X}_k \mathbf{W}_r) + \sigma_k^2\Big] \geq 0, \forall k \in \mathcal{K}, \tag{10-b}$$

$$\text{Tr}(\mathbf{W}_c) + \text{Tr}(\mathbf{W}_r) \leq P_T, \tag{10-c}$$

$$\text{rank}(\mathbf{W}_c) = 1, \text{rank}(\mathbf{W}_r) = 1, \tag{10-d}$$

where

$$\begin{aligned}\mathbf{C} = \int_{\varphi_A - \frac{\Delta\varphi}{2}}^{\varphi_A + \frac{\Delta\varphi}{2}} \int_{\vartheta_A - \frac{\Delta\vartheta}{2}}^{\vartheta_A + \frac{\Delta\vartheta}{2}} \Big[&\mathbf{H}_{BR}^{\text{H}} diag\big(\boldsymbol{\phi}^{\text{H}}\big)\mathbf{a}(\vartheta, \varphi)\mathbf{a}^{\text{H}}(\vartheta, \varphi)\, diag\big(\boldsymbol{\phi}^{\mathbf{H}}\big)\mathbf{H}_{BR} \\ &\mathbf{w}_B \mathbf{w}_B^{\text{H}} \mathbf{H}_{BR}^{\text{H}} diag(\boldsymbol{\phi})\mathbf{a}(\vartheta, \varphi)\mathbf{a}^{\text{H}}(\vartheta, \varphi) diag(\boldsymbol{\phi})\mathbf{H}_{BR} \\ &sin\vartheta\Big] d\vartheta\, d\varphi,\end{aligned} \tag{11}$$

$$\mathbf{X}_k = \Big[\mathbf{h}_{Bk} + \mathbf{H}_{BR}^{\text{H}} \boldsymbol{\Theta}^{\text{H}}(\boldsymbol{\Psi}_R, \boldsymbol{\Psi}_k)\mathbf{h}_{Rk}\Big]\Big[\mathbf{h}_{Bk}^{\text{H}} + \mathbf{h}_{Rk}^{\text{H}} \boldsymbol{\Theta}(\boldsymbol{\Psi}_R, \boldsymbol{\Psi}_k)\mathbf{H}_{BR}\Big], \forall k \in \mathcal{K}, \tag{12}$$

where $\mathbf{W}_c = \mathbf{w}_c \mathbf{w}_c^{\text{H}}$, $\mathbf{W}_r = \mathbf{w}_r \mathbf{w}_r^{\text{H}}$, and $\mu = \frac{\lambda^2 \mathbb{E}\{L_1\}}{64\pi^3 r^2 \sigma_{\text{r}}^2}$, which represents the constant values. To deal with rank one constraint, we leverage SDR technique. By eliminating rank one constraint from the problem formulation, the relaxed problem is given by

$$\text{(P4)}: \underset{\mathbf{w}_c, \mathbf{w}_r}{\text{maximize}}\ \text{SNR}, \tag{13-a}$$

$$\text{subject to}(10-\text{b}),\ (10-\text{c}). \tag{13-b}$$

Problem (P4) is a convex semi-definite programming (SDP), and can be solved efficiently by CVX toolbox. The optimal values of $\mathbf{w}_c$ and $\mathbf{w}_\text{r}$ can be derived by performing eigenvalue decomposition (EVD) on the matrices $\mathbf{W}_c$ and $\mathbf{W}_r$.

3.2 Optimize $\mathbf{w}_B$

With $\mathbf{w}_c$, $\mathbf{w}_r$, and $\boldsymbol{\phi}$ being fixed, the sub-problem can be expressed as

$$(\text{P5}):\ \underset{\mathbf{w}_B}{\text{maximize}}\ \mathbf{w}_B^{\text{H}}\mathbf{M}\mathbf{w}_B, \tag{14-a}$$

$$\text{subject to}\quad \|\mathbf{w}_{B2}=1\|, \tag{14-b}$$

where

$$\begin{aligned}\mathbf{M}=\int_{\varphi_A-\frac{\Delta\varphi}{2}}^{\varphi_A+\frac{\Delta\varphi}{2}}\int_{\vartheta_A-\frac{\Delta\vartheta}{2}}^{\vartheta_A+\frac{\Delta\vartheta}{2}}\Big\{&\tfrac{\lambda^2\mathbb{E}\{L_1\}}{64\pi^3r^2}\,\mathbf{H}_{BR}^{\text{H}}diag(\boldsymbol{\phi})\mathbf{a}(\vartheta,\varphi)\\ &\mathbf{a}^{\text{H}}(\vartheta,\varphi)diag(\boldsymbol{\phi})\mathbf{H}_{BR}(\mathbf{w}_c\mathbf{w}_c^{\text{H}}+\mathbf{w}_r\mathbf{w}_r^{\text{H}})\\ &\mathbf{H}_{BR}^{\text{H}}diag\left(\boldsymbol{\phi}^{\text{H}}\right)\mathbf{a}(\vartheta,\varphi)\mathbf{a}^{\text{H}}(\vartheta,\varphi)diag\left(\boldsymbol{\phi}^{\text{H}}\right)\\ &\mathbf{H}_{BR}sin\vartheta\Big\}d\vartheta\,d\varphi.\end{aligned} \tag{15}$$

The objective function is equivalent to maximize $\frac{w_B^H M w_B}{w_B w_B^H}$ since $\mathbf{w}_B^{\text{H}}\mathbf{w}_B=1$ holds, problem (P5) is a common Rayleigh-quotient problem, and its solution can easily be obtained as

$$\mathbf{w}_B(opt)=\mathbf{v}_{max}\mathbf{M}, \tag{16}$$

in which, $\mathbf{v}_{max}$ denotes the eigenvector of $\mathbf{M}$ corresponds to the largest eigenvalue of $\mathbf{M}$.

3.3 Optimize $\boldsymbol{\phi}$

For a given $\mathbf{w}_c$, $\mathbf{w}_r$, and $\mathbf{w}_B$, the sub-problem can be formulated as

$$(\text{P6}):\ \underset{\boldsymbol{\phi}}{\text{maximize}}\ \text{SNR}, \tag{17-a}$$

$$\text{subject to}(8-\text{c}),\ (8-\text{d}). \tag{17-b}$$

To linearize the objective function, we will employ a real-valued first-order Taylor expansion. Additionally, to convert constraint (8-d) into a linear form, we will utilize the Charnes-Cooper Transformation. Then, the problem will be relaxed by using SDR technique, and SCA-based algorithm will be designed to obtain the optimal solution.

Charnes-Cooper Transformation. To tackle constraint (8-d), we define a vector. $\mathbf{z} = \left[\boldsymbol{\phi}^{\mathrm{T}}, 1\right]^{\mathrm{T}}$, and $\mathbf{Z} = \mathbf{z}\mathbf{z}^{\mathrm{H}}$. Then, we define two new matrices as follow.

$$\mathbf{Q}_{ck} = \begin{bmatrix} diag\left(\mathbf{w}_c^{\mathrm{H}}\mathbf{H}_{BR}^{\mathrm{H}}\right)\mathbf{h}_{Rk}\mathbf{h}_{Rk}^{\mathrm{H}}diag\left(\mathbf{H}_{BR}\mathbf{w}_c\right) & diag\left(\mathbf{w}_c^{\mathrm{H}}\mathbf{H}_{BR}^{\mathrm{H}}\right)\mathbf{h}_{Rk}\mathbf{h}_{Bk}^{\mathrm{H}}\mathbf{w}_c \\ \mathbf{w}_c^{\mathrm{H}}\mathbf{h}_{Bk}\mathbf{h}_{Rk}^{\mathrm{H}}diag\left(\mathbf{H}_{BR}\mathbf{w}_c\right) & \mathbf{w}_c^{\mathrm{H}}\mathbf{h}_{Bk}\mathbf{h}_{Bk}^{\mathrm{H}}\mathbf{w}_c \end{bmatrix}, \forall k \in \mathcal{K}$$

$$\mathbf{Q}_{rk} = \begin{bmatrix} diag\left(\mathbf{w}_r^{\mathrm{H}}\mathbf{H}_{BR}^{\mathrm{H}}\right)\mathbf{h}_{Rk}\mathbf{h}_{Rk}^{\mathrm{H}}diag\left(\mathbf{H}_{BR}\mathbf{w}_r\right) & diag\left(\mathbf{w}_r^{\mathrm{H}}\mathbf{H}_{BR}^{\mathrm{H}}\right)\mathbf{h}_{Rk}\mathbf{h}_{Bk}^{\mathrm{H}}\mathbf{w}_r \\ \mathbf{w}_r^{\mathrm{H}}\mathbf{h}_{Bk}\mathbf{h}_{Rk}^{\mathrm{H}}diag\left(\mathbf{H}_{BR}\mathbf{w}_r\right) & \mathbf{w}_r^{\mathrm{H}}\mathbf{h}_{Bk}\mathbf{h}_{Bk}^{\mathrm{H}}\mathbf{w}_r \end{bmatrix}, \forall k \in \mathcal{K}.$$

Real-Valued First-Order Taylor Expansion. To convexify the objective function, first, we define $f(\boldsymbol{\phi})$ as a function dependent on $\boldsymbol{\phi}$ as follow.

$$\begin{aligned} f(\boldsymbol{\phi}) = \int_{\varphi_A-\frac{\Delta\varphi}{2}}^{\varphi_A+\frac{\Delta\varphi}{2}} \int_{\vartheta_A-\frac{\Delta\vartheta}{2}}^{\vartheta_A+\frac{\Delta\vartheta}{2}} \{ & \mathbf{a}^{\mathrm{H}}(\vartheta,\varphi)diag(\boldsymbol{\phi})\mathbf{H}_{BR}(\mathbf{w}_c\mathbf{w}_c^{\mathrm{H}} + \mathbf{w}_r\mathbf{w}_r^{\mathrm{H}}) \\ & \mathbf{H}_{BR}^{\mathrm{H}}diag\left(\boldsymbol{\phi}^{\mathrm{H}}\right)\mathbf{a}(\vartheta,\varphi)\mathbf{a}^{\mathrm{H}}(\vartheta,\varphi)diag\left(\boldsymbol{\phi}^{\mathrm{H}}\right)\mathbf{H}_{BR} \\ & \mathbf{w}_B\mathbf{w}_B^{\mathrm{H}}\mathbf{H}_{BR}^{\mathrm{H}}diag(\boldsymbol{\phi})\mathbf{a}(\vartheta,\varphi)sin\vartheta\}d\vartheta d\varphi. \end{aligned} \tag{18}$$

Furthermore, we introduce auxiliary matrices that are associated with ϑ and φ as

$$\mathbf{J}(\vartheta,\varphi) = \left[diag\left(\mathbf{a}^{\mathrm{H}}(\vartheta,\varphi)\right)\mathbf{H}_{BR}(\mathbf{w}_c\mathbf{w}_c^{\mathrm{H}} + \mathbf{w}_r\mathbf{w}_r^{\mathrm{H}})\mathbf{H}_{BR}^{\mathrm{H}}diag(\mathbf{a}(\vartheta,\varphi))\right]^{\mathrm{T}}, \tag{19}$$

$$\mathbf{H}(\vartheta,\varphi) = diag\left(\mathbf{a}^{\mathrm{H}}(\vartheta,\varphi)\right)\mathbf{H}_{BR}\mathbf{w}_B\mathbf{w}_B^{\mathrm{H}}\mathbf{H}_{BR}^{\mathrm{H}}diag(\mathbf{a}(\vartheta,\varphi))sin\vartheta. \tag{20}$$

Then $f(\boldsymbol{\phi})$ can be expressed as

$$\begin{aligned} f(\boldsymbol{\phi}) &= \int_{\varphi_A-\frac{\Delta\varphi}{2}}^{\varphi_A+\frac{\Delta\varphi}{2}} \int_{\vartheta_A-\frac{\Delta\vartheta}{2}}^{\vartheta_A+\frac{\Delta\vartheta}{2}} \boldsymbol{\phi}^{\mathrm{H}}\mathbf{J}(\vartheta,\varphi)\boldsymbol{\phi}\boldsymbol{\phi}^{\mathrm{H}}\mathbf{H}(\vartheta,\varphi)\boldsymbol{\phi}d\vartheta d\varphi, \\ f(\boldsymbol{\phi}) &= \int_{\varphi_A-\frac{\Delta\varphi}{2}}^{\varphi_A+\frac{\Delta\varphi}{2}} \int_{\vartheta_A-\frac{\Delta\vartheta}{2}}^{\vartheta_A+\frac{\Delta\vartheta}{2}} \mathbf{z}^{\mathrm{H}}\tilde{\mathbf{J}}(\vartheta,\varphi)\mathbf{z}\mathbf{z}^{\mathrm{H}}\tilde{\mathbf{H}}(\vartheta,\varphi)\mathbf{z}d\vartheta d \\ &= f(\mathbf{z}), \end{aligned} \tag{21}$$

where

$$\tilde{\mathbf{J}}(\vartheta,\varphi) = \begin{bmatrix} \mathbf{J}(\vartheta,\varphi) & 0_{N\times 1} \\ 0_{1\times N} & 0 \end{bmatrix} \text{ and } \tilde{\mathbf{H}}(\vartheta,\varphi) = \begin{bmatrix} \mathbf{H}(\vartheta,\varphi) & 0_{N\times 1} \\ 0_{1\times N} & 0 \end{bmatrix}, \tag{22}$$

we have

$$\mathbf{R}(\vartheta,\varphi) = \tilde{\mathbf{J}}^{\mathrm{T}}(\vartheta,\varphi) \otimes \tilde{\mathbf{H}}(\vartheta,\varphi) \text{ and } \mathbf{S}(\vartheta,\varphi) = \int_{\varphi_A-\frac{\Delta\varphi}{2}}^{\varphi_A+\frac{\Delta\varphi}{2}} \int_{\vartheta_A-\frac{\Delta\vartheta}{2}}^{\vartheta_A+\frac{\Delta\vartheta}{2}} \mathbf{R}(\vartheta,\varphi)d\vartheta d\varphi.$$

Then

$$f(\mathbf{z}) = \left\| \left(\mathbf{z}^{\mathrm{T}} \otimes \mathbf{z}^{\mathrm{H}} \right) \mathbf{U} \Lambda^{1/2} \right\|_2^2,$$

By utilizing the EVD on $\mathbf{S}$

$$f(\mathbf{z}) = \left\| \left(\mathbf{z}^{\mathrm{T}} \otimes \mathbf{z}^{\mathrm{H}} \right) \mathbf{U} \Lambda^{1/2} \right\|_2^2,$$

where $\mathbf{U}\Lambda^{1/2} = \left[\boldsymbol{\delta}_1, ..., \boldsymbol{\delta}_{(N+1)^2} \right]$, and $\boldsymbol{\delta}_\iota$ is the ι-th column of $\mathbf{U}\Lambda^{1/2}$. The function $f(\mathbf{z})$ can be rewritten as

$$f(\mathbf{z}) = \mathbf{v}(\mathbf{Z})_2^2, \tag{23}$$

where $\mathbf{v}(\mathbf{Z})$ is a vector with regard to $\mathbf{Z}$, defined as

$$\left[\mathrm{Tr}(\mathbf{B}_1 \mathbf{Z}), \mathrm{Tr}(\mathbf{B}_2 \mathbf{Z}), ..., \mathrm{Tr}(\mathbf{B}_{(N+1)^2} \mathbf{Z} \right]^{\mathrm{T}}, \tag{24}$$

where $\mathbf{B}_\iota = \mathrm{vec}^{-1}(\boldsymbol{\delta}_\iota)$, for $\iota = 1, 2, ..., (N+1)^2$.

The sub-problem (P6) can be recast as

$$(\mathrm{P7}): \underset{\mathbf{Z} \succcurlyeq 0}{\text{maximize}} \ \|\mathbf{v}(\mathbf{Z})\|_2^2, \tag{25-a}$$

$$\text{subject to } \mathrm{Tr}(\mathbf{E}_n \mathbf{Z}) = 1, n = 1, 2, .., N+1, \tag{25-b}$$

$$\mathrm{Tr}(\mathbf{Q}_{ck} \mathbf{Z}) - \gamma \left[\mathrm{Tr}(\mathbf{Q}_{rk} \mathbf{Z}) + \sigma_k^2 \right] \geq 0, \forall k \in \mathcal{K}, \tag{25-c}$$

$$\text{rank } (\mathbf{Z}) = 1, \tag{25-d}$$

where $\mathbf{E}_n$ is a selective matrix satisfying

$$[\mathbf{E}_n]_{(m,\ell)} = \begin{cases} 1, m = \ell = n, \\ 0, \textit{otherwise}. \end{cases} \tag{26}$$

We suggest using first-order Taylor expansion to make (P7) even more convex. $\mathcal{H}_{\mathbf{q}_x}((\hbar(\mathbf{q}))$of a function $\hbar(\mathbf{q})$around $\mathbf{q}_x$, which is stated as

$$\mathcal{H}_{\mathbf{q}_x}((\hbar(\mathbf{q})) = \hbar(\mathbf{q}_x) + \langle \frac{\partial \hbar(\mathbf{q})}{\partial \mathbf{q}} |_{\mathbf{q}=\mathbf{q}_x}, (\mathbf{q} - \mathbf{q}_x) \rangle. \tag{27}$$

To find the first-order Taylor expansion of the objective function around $\mathbf{v}(\mathbf{Z}_x)$, we can use the following equation

$$\mathcal{H}_{\mathbf{v}(\mathbf{Z}_x)} \left(\mathbf{v}(\mathbf{Z})_2^2 \right) = \mathbf{v}(\mathbf{Z}_x)_2^2 + \frac{\partial \mathbf{v}(\mathbf{Z})_2^2}{\partial \mathbf{v}(\mathbf{Z})} |_{\mathbf{v}(\mathbf{Z})=\mathbf{v}(\mathbf{Z}_x)}, [(\mathbf{v}(\mathbf{Z}) - \mathbf{v}(\mathbf{Z}_x)]. \tag{28}$$

A real representation $\mathcal{H}_{\mathbf{v}(\mathbf{Z}_x)}\left(\mathbf{v}(\mathbf{Z})_2^2\right)$ can be obtained through the following derivation

$$\mathcal{H}_{\tilde{\mathbf{v}}(\mathbf{Z}_x)}\left(\tilde{\mathbf{v}}(\mathbf{Z})_2^2\right) = \mathrm{Tr}\left(\boldsymbol{\zeta}_{\mathbf{Z}_x}\mathbf{Z}\right), \tag{29}$$

where $\tilde{\mathbf{v}}(\mathbf{Z})$ is a real-valued vector, and $\boldsymbol{\zeta}_{\mathbf{Z}_x}$ is derived as

$$\zeta_{\mathbf{Z}_x} = \frac{1}{2\|\tilde{\mathbf{v}}(\mathbf{Z})\|_2^2}\left\{\sum_{\iota=1}^{(N+1)^2}\mathrm{Tr}\left(\left(\mathbf{B}_\iota + \mathbf{B}_\iota^{\mathrm{H}}\right)\mathbf{Z}_x\right)\left(\mathbf{B}_\iota + \mathbf{B}_\iota^{\mathrm{H}}\right) - \sum_{\iota=1}^{(N+1)^2}\mathrm{Tr}\left(\left(\mathbf{B}_\iota - \mathbf{B}_\iota^{\mathrm{H}}\right)\mathbf{Z}_x\right)\left(\mathbf{B}_\iota - \mathbf{B}_\iota^{\mathrm{H}}\right)\right\},$$

where

$$\|\tilde{\mathbf{v}}(\mathbf{Z})\|_2^2 = \mathrm{Tr}(\frac{1}{2}\left(\left(\mathbf{B}_\iota + \mathbf{B}_\iota^{\mathrm{H}}\right)\mathbf{Z}_x\right))^2 + \mathrm{Tr}(\frac{-j}{2}\left(\left(\mathbf{B}_\iota - \mathbf{B}_\iota^{\mathrm{H}}\right)\mathbf{Z}_x\right))^2.$$

As a result of the proof which is outlined in [10, Appendix B], $\mathcal{H}_{\mathbf{v}(\mathbf{Z}_x)}\left(\|\mathbf{v}(\mathbf{Z})\|_2^2\right)$ is equivalent to $\mathcal{H}_{\tilde{\mathbf{v}}(\mathbf{Z}_\mathbf{x})}\left(\|\tilde{\mathbf{v}}(\mathbf{Z})\|_2^2\right)$ and can be utilized as a surrogate function of $\|\mathbf{v}(\mathbf{Z})\|_2^2$. Accordingly, the objective function can be modified as

$$(\mathrm{P8}):\ \underset{\mathbf{Z}\succcurlyeq 0}{\mathrm{maximize}}\ \mu\mathrm{Tr}\left(\boldsymbol{\zeta}_{\mathbf{Z}_x}\mathbf{Z}\right), \tag{30-a}$$

$$\mathrm{subject\ to}(25-\mathrm{b}),\ (25-\mathrm{c}),\ (25-\mathrm{d}). \tag{30-b}$$

SCA-Based Algorithm. A SCA-based algorithm will iteratively solve (P8) to approach the solution of (P7), then the SDR technique can be employed to relax the rank-one constraint. In the event that a rank-one solution is obtained, we can utilize the EVD to acquire the optimal values of $\mathbf{z}$ and $\boldsymbol{\phi}$.

4 Simulation Results

In this section, simulations are conducted to validate the proposed algorithm's analytical properties and assess our beamforming design's performance. The locations of the BS and the IRS are [0,0,18] and [2,10,12] meters, and the locations of the k-th users, in which K = 3, are [20,80,25], [20,80,15], and [–20,80,10] meters, respectively. The elevation and azimuth angle spread of the scattering surface area A($\Delta\vartheta$, $\Delta\varphi$) are $\Delta\varphi = \frac{\pi}{16}$;$r$ = 8 m. The noise powers are $\sigma_r^2 = -90$ dBm and $\sigma_k^2 = -80$ dBm, which the latter considered equal for all CUs. The signal wavelength is $\lambda = 11.9$ cm; the average scattering loss is $\mathbb{E}\{\mathrm{L}_1\} = -10$ dBm; the antenna element spacing is $= \frac{\lambda}{2}$; the SINR threshold is $\gamma = 0.9$; the termination condition for the algorithm is $\in= 0.0002$; the Rician factor is $\kappa = 10$; the path loss exponents for BS-IRS, IRS-k, and BS-k links are $\alpha BR = 2.2$, $\alpha Rk = 2.3$, and $\alpha Bk = 2.5$; the path loss coefficient is $L_0 = -30$ dB; the total transmit power limit is $P_T = 30$ dBm. During the simulations, the values of M and N will vary based on different scenarios. The CVX Toolbox with the Sedumi solver is employed to solve the optimization problems. For the computational of the integrals, we utilize the trapezoidal method, which involves approximating the integral value by dividing the variable range into 100 divisions. This approach ensures a high level of accuracy in the approximation of the integral.

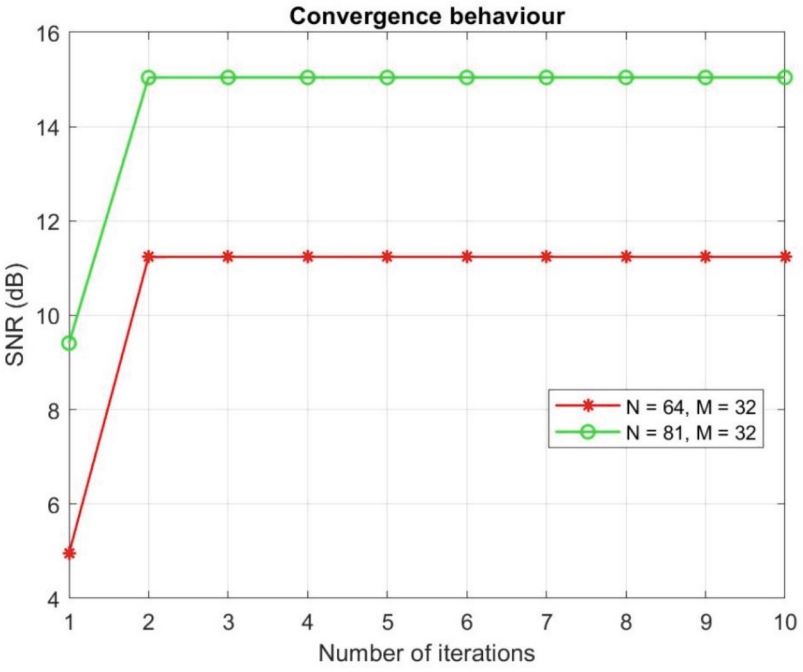

Fig. 2. Convergence behavior of the algorithm at N = 64 and N = 81.

Considering the aforementioned parameters, Fig. 2 demonstrates the convergence behavior of our proposed algorithm; we can observe that the algorithm exhibits fast convergence and the impact of increasing the number of IRS elements on the convergence behavior.

Figure 3 illustrates the relationship between the number of IRS elements and the SNR values considering different numbers of BS antennas. By analyzing the curves, we can notice that the SNR values tend to improve as the number of IRS elements increases.

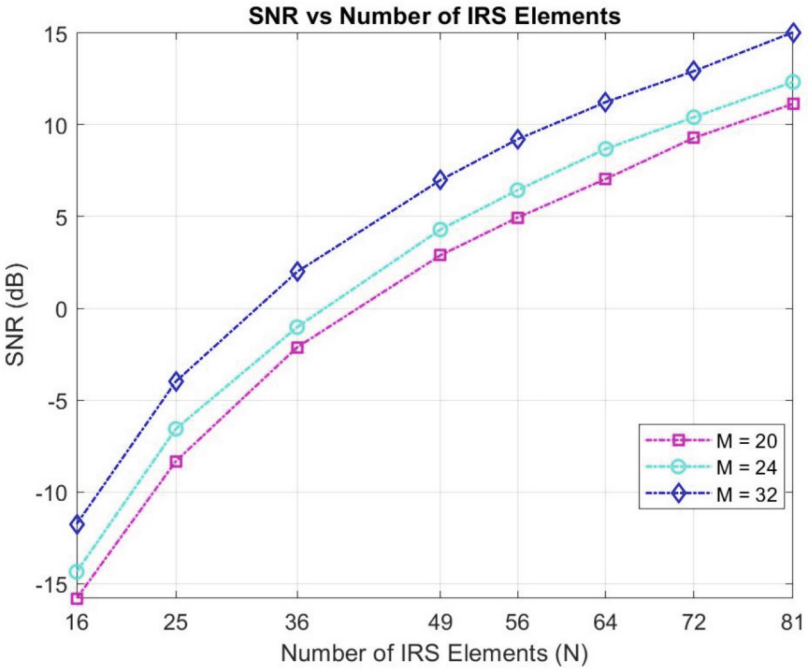

Fig. 3. SNR at the BS vs N at M = 20, M = 24, and M = 32.

Furthermore, increasing the number of BS antennas leads to increased SNR values.

In Fig. 4, the SNR values are plotted against varying transmit power levels by comparing the SNR values obtained from our proposed algorithm and the SNR values from the matched filter, where $\mathbf{w}_c$, $\mathbf{w}_r$, and $\mathbf{w}_B$ are derived as $\mathbf{w}_c = \mathbf{w}_r = \mathbf{w}_B = \beta \mathbf{a}^{\mathrm{H}}(\vartheta_{BR}, \varphi_{BR})$, and the IRS elements are randomly generated. The curves clearly demonstrate that the SNR values obtained from our algorithm consistently exhibit higher values compared to those obtained from the matched filter.

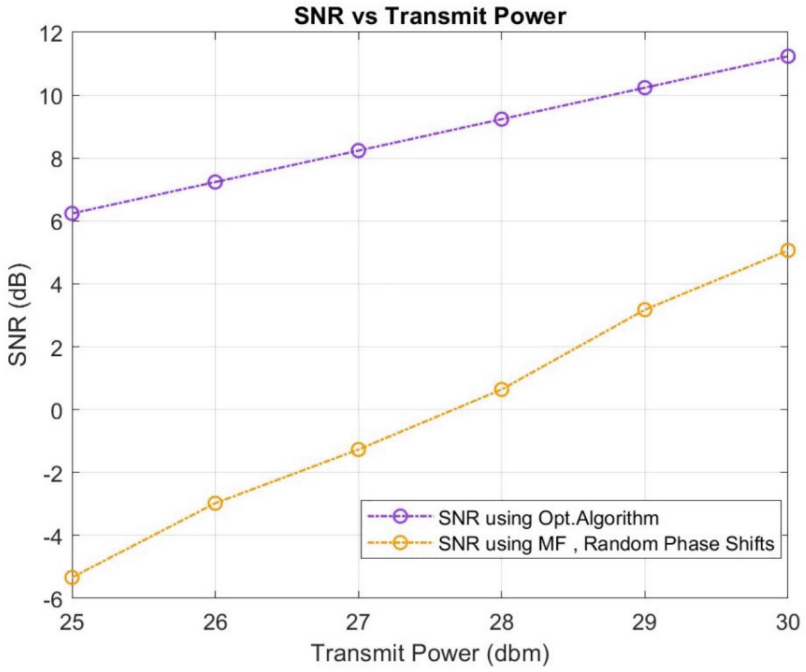

Fig. 4. SNR at the BS with respect to P_T, when using our algorithm and MF at M = 32 and N = 64.

The depicted scenario in Fig. 5, discusses the comparison between the SNR values acquired from our algorithm and the matched filter at corresponding transmit power levels when considering the fixed total number of N and M, the figure sheds.

light on our algorithm's advantages and potential benefits by showcasing the higher SNR values it achieves compared to the MF approach.

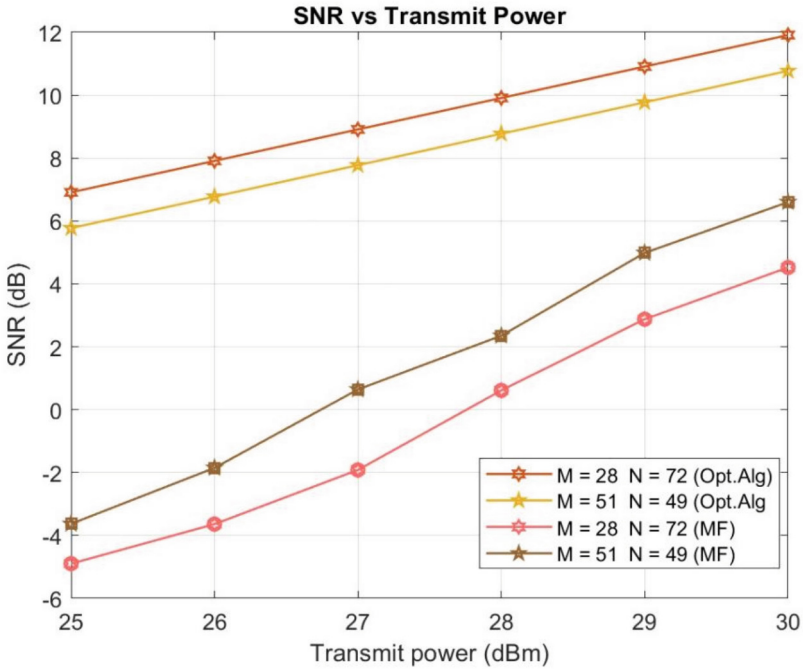

Fig. 5. SNR at the BS and P_T with a fixed total of M + N = 100 for our algorithm compared with MF.

5 Conclusion

In this article, the integration of IRS in the ISAC system, with its ability to reconfigure the wireless propagation environment and by leveraging active and passive beamforming approach, offer significant advantages in maximizing the SNR at the BS, further enhancing target detection. An optimization problem is formulated to maximize the SNR at the BS while ensuring the minimum SINR at each communication user. The optimization variables are decoupled by employing alternating optimization, and the intractable problem is split into three sub-problems. Simulation results highlight the effectiveness and superiority of our algorithm in maximizing the SNR at the BS compared to the benchmark scheme, thereby opening up opportunities for improved capabilities and expanded applications.

Acknowledgment. This work was sponsored by the National Natural Science Foundation of China under Grant 62271352, the Shanghai Science and Technology Innovation Action Plan Project No. 21220713100, the Natural Science Foundation of Shanghai under Grant 22ZR1465100, and the Shanghai Automobile Foundation under Grant 1905.

References

1. Abeywickrama, S., Zhang, R., Wu, Q., Yuen, C.: Intelligent reflecting surface: practical phase shift model and beamforming optimization. IEEE Trans. Commun. **68**(9), 5849–5863 (2020)
2. Huang, C., Zappone, A., Alexandropoulos, G.C., Debbah, M., Yuen, C.: Reconfigurable intelligent surfaces for energy efficiency in wireless communication. IEEE Trans. Wirel. Commun. **18**(8), 4157–4170 (2019)
3. Patil, A., et al.: A comprehensive survey on spectrum sharing techniques for 5G/B5G intelligent wireless networks: opportunities, challenges and future research directions (2022). https://doi.org/10.48550/arXiv.2211.08956
4. Ahmed, A., Zhang, Y.D., Himed, B.: Distributed dual-function radar-communication MIMO system with optimized resource allocation. In: 2019 IEEE Radar Conference (RadarConf), Boston, MA, USA, pp. 1–5 (2019)
5. Ma, D., Shlezinger, N., Huang, T., Liu, Y., Eldar, Y.C.: Joint radar-communication strategies for autonomous vehicles: combining two key automotive technologies. IEEE Signal Process. Mag. **37**(4), 85–97 (2020)
6. Yan, S., Cai, S., Xia, W., Zhang, J., Xia, S.: A reconfigurable intelligent surface aided dual-function radar and communication system. In: 2022 2nd IEEE International Symposium on Joint Communications & Sensing (JC&S), pp. 1–6 (2022)
7. Wang, X., Fei, Z., Zheng, Z., Guo, J.: Joint waveform design and passive beamforming for RIS-assisted dual-functional radar-communication system. IEEE Trans. Veh. Technol. **70**(5), 5131–5136 (2021)
8. Zuo, J., Liu, Y., Zhu, C., Zou, Y., Zhang, D., Al-Dhahir, N.: Exploiting NOMA and RIS in integrated sensing and communication. IEEE Trans. Veh. Technol. **72**(10), 12941–12955 (2023)
9. Zheng, B., Zhang, R.: Intelligent reflecting surface-enhanced OFDM: channel estimation and reflection optimization. IEEE Wirel. Commun. Lett. **9**(4), 518–522 (2020)
10. Xing, Z., Wang, R., Yuan, X.: Joint active and passive beamforming design for reconfigurable intelligent surface enabled integrated sensing and communication. IEEE Trans. Commun. **71**(4), 2457–2474 (2023)